Temperature-Sensitive Alleles of *RSW2* Link the KORRIGAN Endo-1,4-β-Glucanase to Cellulose Synthesis and Cytokinesis in Arabidopsis[1]

Diana R. Lane[2], Allison Wiedemeier, Liangcai Peng[3], Herman Höfte, Samantha Vernhettes, Thierry Desprez, Charles H. Hocart, Rosemary J. Birch, Tobias I. Baskin, Joanne E. Burn, Tony Arioli[4], Andreas S. Betzner, and Richard E. Williamson*

Plant Cell Biology Group, Research School of Biological Sciences, Australian National University, P.O. Box 475, Canberra, Australian Capital Territory 2601, Australia (D.R.L., L.P., C.H.H., R.J.B., J.E.B., T.A., R.E.W.); University of Missouri, Biological Sciences, Missouri 65211–7400 (A.W., T.I.B.); Laboratoire de Biologie Cellulaire, Institut National de la Recherche Agronomique, Route de St–Cyr, 78026 Versailles cedex, France (H.H., S.V., T.D.); and Groupe Limagrain Pacific Proprietary Limited, P.O. Box 475, Canberra (A.S.B.)

An 8.5-kb cosmid containing the *KORRIGAN* gene complements the cellulose-deficient *rsw2-1* mutant of Arabidopsis. Three temperature-sensitive alleles of *rsw2* show single amino acid mutations in the putative endo-1,4-β-glucanase encoded by *KOR*. The F_1 from crosses between *kor-1* and *rsw2* alleles shows a weak, temperature-sensitive root phenotype. The shoots of *rsw2-1* seedlings produce less cellulose and accumulate a short chain, readily extractable glucan resembling that reported for *rsw1* (which is defective in a putative glycosyltransferase required for cellulose synthesis). The double mutant (*rsw2-1 rsw1*) shows further reductions in cellulose production relative to both single mutants, constitutively slow root growth, and enhanced temperature-sensitive responses that are typically more severe than in either single mutant. Abnormal cytokinesis and severely reduced birefringent retardation in elongating root cell walls of *rsw2* link the enzyme to cellulose production for primary cell walls and probably cell plates. The Rsw2$^-$ phenotype generally resembles the Kor$^-$ and cellulose-deficient Rsw1$^-$ phenotypes, but anther dehiscence is impaired in Rsw2-1$^-$. The findings link a second putative enzyme activity to cellulose synthesis in primary cell walls of Arabidopsis and further increases the parallels to cellulose synthesis in *Agrobacterium tumefaciens* where the *celA* and *celC* genes are required and encode a putative glycosyltransferase and an endo-1,4-β-glucanase related to RSW1 and KOR, respectively.

Cellulose is a key cell wall polysaccharide whose production impinges on many aspects of plant biology. Enzymology has enjoyed little success in elucidating the processes by which it is synthesized, but mutants have recently begun to point to some of the genes required. Two genes (*RADIAL SWELLING1*, Arioli et al., 1998; *IRREGULAR XYLEM3*, Taylor et al., 1999) of Arabidopsis have been linked to cellulose production through cellulose-deficient mutants. Both genes encode putative glycosyltransferases that are related to the product of the *celA* gene of cotton (Pear et al., 1996). They are members of a subgroup of a large and complex family of related sequences (Richmond and Somerville, 2000). Two other nonallelic radial swelling mutants (*rsw2* and *rsw3*) show very similar polysaccharide changes to those seen in *rsw1*, that is changes in cellulose levels greatly exceed changes in other polysaccharides (Peng et al., 2000). The *RSW2* and *RSW3* genes could encode further glycosyltransferases or gene products with distinct functions not previously linked to cellulose synthesis. We show here that *RSW2* is allelic to *KORRIGAN*, a gene that encodes a putative membrane-bound endo-1,4-β-glucanase (Nicol et al., 1998; Zuo et al., 2000). The endoglucanase has previously been linked to cell expansion through the weak *kor-1* allele (Nicol et al., 1998), and more recently it has also been linked to cytokinesis by the stronger *kor-2* allele (Zuo et al., 2000). Three temperature-sensitive alleles of *rsw2* with single amino acid substitutions in the coding region of KOR show cytokinesis and cell expansion abnormalities and, most importantly, morphological, and chemical data strongly point to the endoglucanase having an important role in depositing cellulose in primary cell walls.

[1] This work was supported by an Australian Postgraduate Award (Industry, to D.R.L.), by a Patricia Roberts Harris Fellowship (to A.W.), by a Cotton Research and Development Corporation Fellowship (to J.E.B.), and by a U.S. Department of Energy grant (award no. 94ER20146 to T.I.B.) that does not constitute endorsement by that department of views expressed herein.

[2] Present address: Cellular and Structural Biology, University of Colorado Health Sciences Center, B–111 4200 E. 9th Avenue, Denver, CO 80262.

[3] Present address: The Plant Gene Expression Center, U.S. Department of Agriculture/Agricultural Research Service, University of California/Berkeley, 800 Buchanan Street, Albany, CA 94710.

[4] Present address: Aventis Pty Ltd, G.P.O. Box 1600, Canberra, ACT 2601, Australia

* Corresponding author: e-mail richard@rsbs.anu.edu.au; fax 61–2–6249–4331.

RESULTS

Molecular and Genetic Analysis

Three independently isolated lines from the same mutant screen (Baskin et al., 1992) were assigned to the *rsw2* complementation group after crossing to *rsw2-1* produced an F_1 that showed temperature sensitive radial swelling that was essentially indistinguishable from that of each parent. Segregation ratios for the F_2 progeny from crossing *rsw2-1* with the W9 marker line linked the *RSW2* locus to *yi* on the lower part of chromosome 5. Molecular analysis of an F_2 mapping population from a Columbia/Landsberg *erecta* cross placed *rsw2* between *DFR* (5 from 20 plants recombined) and *LFY* (11 from 20), an interval of approximately 30 cM. Only one nga 129/*rsw2* recombinant was detected in 276 F_2 plants, placing *rsw2* nominally 0.2 cM from nga 129. Neighboring markers in the recombinant plant placed *rsw2* south of nga 129. This is close to *KOR,* which lies on the yeast artificial chromosomes CIC 4G5 and CIC 8D5 (Nicol et al., 1998), which mainly extend south of nga 129. Genome sequence now places KOR approximately 60 kb south of nga 129.

Allelism of *rsw2* and *kor* is supported by three observations. First, an 8.5-kB cosmid containing *KOR* (Nicol et al., 1998) restored the $Rsw2^+$ phenotype to *rsw2-1* seedlings (Fig. 1A) and corrected the other features of the phenotype described below. Second, sequencing *KOR* in *rsw2-1, rsw2-3,* and *rsw2-4* showed that each had an independent mutation in which a small aliphatic or hydroxy amino acid is replaced by a larger basic amino acid or amide (Gly-429 to Arg in *rsw2-1*; Ser-183 to Asn in *rsw2-3*; Gly-344 to Arg in *rsw2-4*; *rsw2-2,* although believed to be an independent isolate, proved to have an identical nucleotide change to that in *rsw2-1.*) Third, the F_1 from crossing *rsw2-1* and *kor-1* when transferred to 31°C showed reduced elongation, clustering of root hairs, and slight radial swelling relative to the F_1 from a *kor-1*/Columbia cross (Fig. 1B). Similar results were obtained with the F_1 from crosses between *kor-1* and *rsw2-3* or *rsw2-4*. We will continue to refer to the mutants using the *rsw2* nomenclature (Baskin et al., 1992) but refer to them as mutated in *KOR* and defective in the KOR endo-1,4-β-glucanase (Nicol et al., 1998).

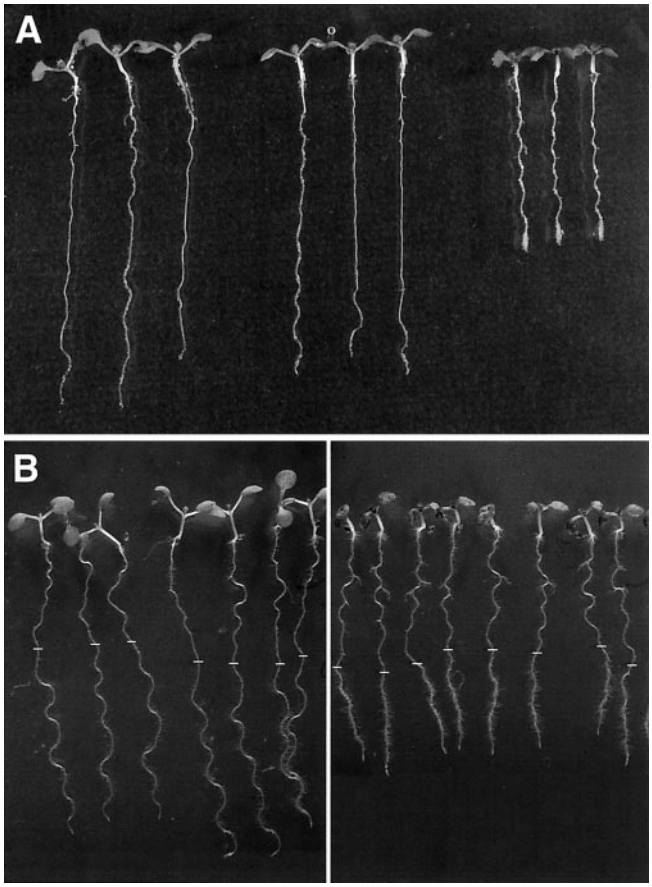

Figure 1. A, Seedlings of *rsw2-1* transformed with an 8.5-kb cosmid containing the *KOR* gene do not show radial swelling when transferred to 31°C for 2 d after 5 d at 20°C. From the left: wild type, *rsw2-1* transformed with *KOR,* and *rsw2-1*. B, F_1 plants from crossing *kor-1* and Columbia wild type (left) compared with F_1 plants from crossing *kor-1* and *rsw2-1*. Growth for 5 d at 20°C (when the position of the root tip was marked) and 2 d at 31°C. The *kor-1*/*rsw2-1* plants show reduced elongation at 31°C (with accompanying clustering of root hairs) and a slight increase in diameter. Hypocotyls and petioles are also shorter.

rsw2 Makes Less Acid-Insoluble Cellulose But Accumulates a Readily Extracted β-1,4-Glucan in Its Shoots

rsw2, like *rsw1,* makes less cellulose in its roots (Peng et al., 2000) and shoots (not shown). We next determined whether *rsw2* also accumulates a novel form of readily extractable β-1,4-glucan in its shoots so further resembling the *rsw1* mutant (Arioli et al., 1998). (Note that, as mentioned in earlier work [Peng et al., 2000], neither *rsw1* nor *rsw2* accumulates glucan in their roots. The reasons for the root/shoot differences are not understood.) The ammonium oxalate, 0.1 M and 4 M KOH fractions from *rsw2* contain much more Glc than do those from wild type when seedlings are grown at 31°C (Table I). Exactly as with *rsw1* (Arioli et al., 1998), a glucan is recovered from the *rsw2* samples by precipitating the charged pectins with cetyl-trimethyl-ammonium bromide (CTAB) from the ammonium oxalate fraction. Much smaller quantities pellet from the two alkali fractions after they have been neutralized and dialyzed. Only Glc is detected as an alditol acetate after trifluoroacetic acid (TFA) hydrolysis of the glucan, and only partially methylated alditol acetates corresponding to t-Glc and 4-Glc are seen after methylation analysis (Fig. 2). (The peaks between t-Glc and 4-Glc seen after amplifying that part of the chromatogram are not carbohydrate material and were not identified when compared with a library of mass spectra.) The t-Glc:4-Glc

Table I. *Monosaccharide composition (nmol mg^{-1} tissue dry wt) of the ammonium oxalate, 0.1 M KOH and 4 M KOH fractions prepared from shoots of wild-type and rsw2-1 seedlings grown at 21°C for 7 d or at 21°C for 2 d and 31°C for 5 d*

Fraction	Genotype		UA[a]	Glc	Gal	Man	Xyl	Ara	Rha	Fuc
Ammonium oxalate	Wild type	21°C	192	42	12	1	9	17	15	2
		31°C	241	80	16	1	8	31	17	2
	rsw2	21°C	204	20	10	1	6	15	11	1
		31°C	239	184	25	2	13	38	22	2
0.1 M KOH	Wild type	21°C	17	2	5	nd[b]	2	7	5	nd
		31°C	17	6	6	nd	2	6	4	nd
	rsw2	21°C	14	5	7	nd	2	8	5	nd
		31°C	15	28	5	nd	2	6	3	nd
4 M KOH	Wild type	21°C	10	29	12	9	26	13	1	3
		31°C	6	52	16	10	22	10	tr[c]	4
	rsw2	21°C	12	38	16	7	23	16	1	3
		31°C	9	122	6	6	23	19	tr	2

[a] UA, Total uronic acids by spectrophotometric assay. [b] nd, Not detected (<0.5 nmol mg^{-1} dry wt). [c] tr, Between 0.5 and 1 nmol mg^{-1} dry wt.

ratio exceeds that seen with acid insoluble cellulose consistent with the readily extracted glucan having shorter chains. Endo-β-1,4-glucanase releases 64% ($n = 4$; relative SD 27%) of the Glc released by TFA, whereas α-amylase released no detectable Glc. The glucan is therefore β-1,4-linked and not derived from any starch that does not extract with dimethylsulfoxide. No glucan can be purified from wild type by the same methods.

In a *rsw1rsw2-1* double mutant, cellulose deposition (measured as TFA-insoluble Glc in whole seedlings grown at 29°C) is reduced below the levels seen in either single mutant (46 ± 2 nmol mg^{-1} tissue dry weight for *rsw1rsw2-1*; 59 ± 2 nmol mg^{-1} dry weight for *rsw1*; 68 ± 2 nmol mg^{-1} dry weight for *rsw2-1*; 89 ± 5 nmol mg^{-1} dry weight for wild type (mean ± SE, $n = 6$). All pairwise combinations were significantly different for $P < 0.01$ according to the Student's t test.

Changes in the Root Growth Zone

Lowered levels of acid-insoluble cellulose (Peng et al., 2000) and accumulation of a readily extracted glucan support the view that cellulose synthesis requires the KOR endo-1,4-β-glucanase (mutated in *rsw2*) as well as the RSW1 glycosyltransferase. We used polarized-light microscopy to investigate whether the amount of cellulose decreased in walls of the root growth zone, a finding to be expected if KOR is needed to make cellulose in primary cell walls and if the defects in KOR cause the radial swelling observed in the mutants. Cell walls appeared darker than background with the compensator optical axis perpendicular to the microfibril optical axis in all tissues of wild-type roots (Fig. 3A) and of *rsw2-4* roots grown at 19°C (Fig. 3B), whereas at 30°C only the epidermis of the mutant was still darker (Fig. 3C). Retardation of epidermal and cortical walls were similar when *rsw2-1* and wild type were grown at 19°C (Fig. 3D) but fell in cortical cell walls after growing the mutant for 12 h at 30°C (Fig. 3E). Epidermal cell walls were unaffected. Although not quantified, retardation in both endodermis and stele of mutants was also lower than retardation in those tissues in wild type, and similar results were obtained with *rsw2-3* and *rsw2-4*.

The quantity of microfibrils and/or their degree of alignment therefore decreased in tissues interior to the epidermis and alterations to the mutant's growth should reflect those changes. We found that all tissues swell at 30°C in both *rsw2-3* and *rsw2-4* and that *rsw2-3* has some constitutive swelling (Fig. 3F). The area changes translate into radial epidermal walls increasing in size by only 40% in *rsw2-4*, whereas radial walls in the cortex and endodermis increased by 161% and 114%, respectively.

The partially constitutive *rsw2-3* had extra cells in the epidermis (38 ± 1 versus 22 ± 1 in wild type; mean ± SE, $n = 16$), cortex (19 ± 2 versus 8 ± 0), endodermis (15 ± 2 versus 9 ± 0), and stele (72 ± 3 versus 48 ± 2) when grown at 19°C (Fig. 4, A and B). Additional cells formed at 31°C, giving both *rsw2-3* and *rsw2-4* a highly disorganized appearance with wavy and sometimes incomplete cell walls (Fig. 4, C and D).

Other Features of the Phenotype

A temperature-sensitive phenotype is seen in many parts of *rsw2-1* plants. Most features were described for the leaky insertional mutant *kor-1* (Nicol et al., 1998): Hypocotyls swelled subapically when transferred at d 3 from 21°C to 31°C in the dark but light grown hypocotyls were less obviously affected; cotyledons and subsequent leaves were smaller with simpler shaped pavement cells; bolts were shorter, flowers more clustered, and floral morphology abnormal on plants transferred to 31°C after bolting began. Sepals and petals are smaller than wild type

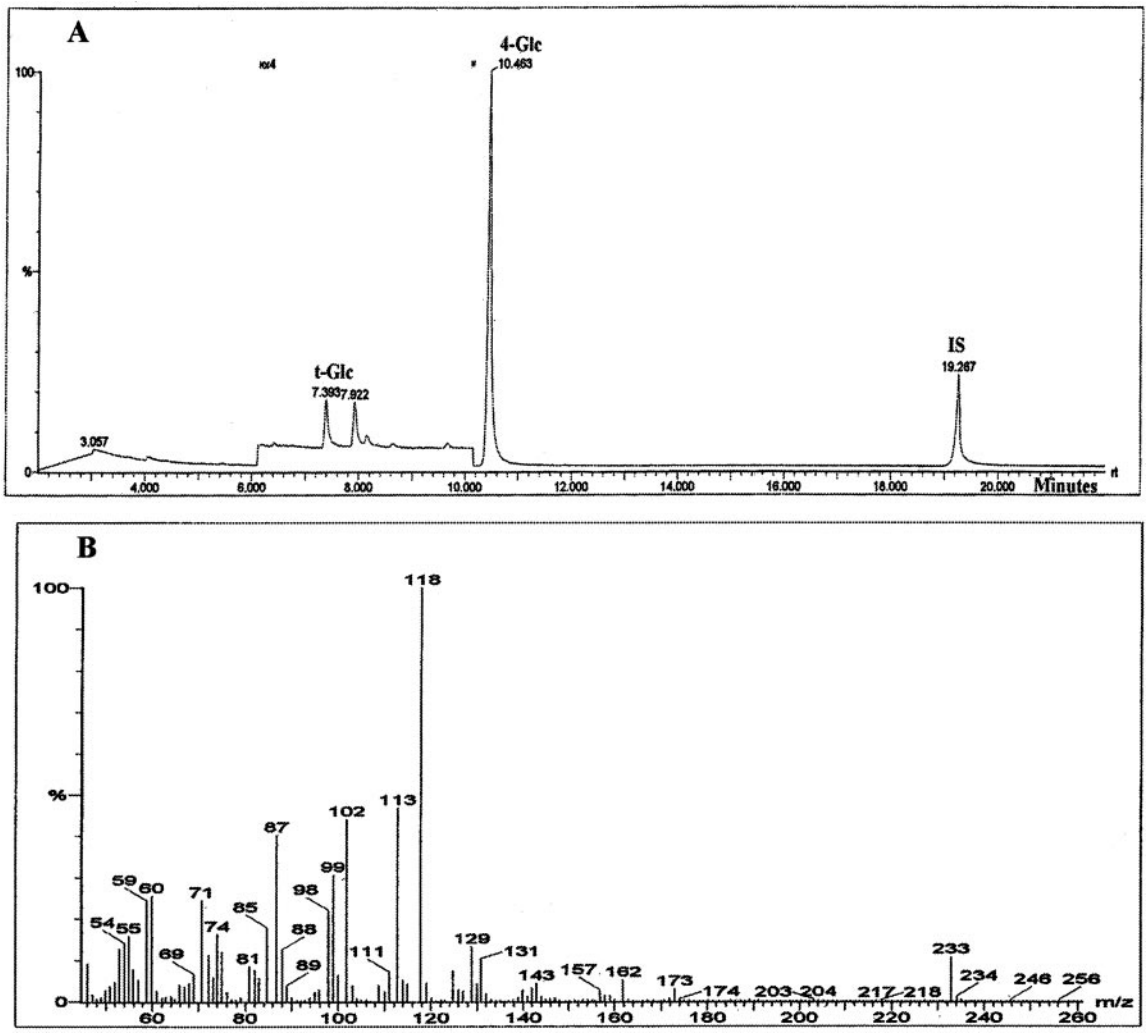

Figure 2. Properties of the readily extracted glucan pooled after purification from ammonium oxalate, 0.1 M KOH, and 4-M KOH fractions from whole *rsw2-1* seedlings. A, GC/MS chromatogram of partially methylated alditol acetates from methylation analysis of the glucan. The peaks are assigned to t-Glc and 4-Glc by comparing retention time and mass spectrum with standards derived from undermethylation of appropriate methylglycosides. The chromatogram's vertical scale is enlarged ×4 between the arrowheads to show that no peaks corresponding to other linkages are detected. Unlabeled peaks visible after enlargement are not carbohydrate material and were not identified by comparison with a library of mass spectra. IS indicates the internal standard, *myo*-inositol. Retention times are in min. B, Mass spectra for the peak marked 4-Glc and showing ions such as 102, 113, 118, 162, and 233 expected from fragmentation of 1,4,5-tri-*O*-acetyl-(1-deuterio)-2,3,6-tri-*o*-methyl glucitol (Carpita and Shea, 1989).

so that the pistil often protrudes beyond them when the stigma is receptive (Fig. 5A). The pistil itself often appeared distorted. The mixture of long and short cells in the epidermis of wild-type sepals was much less marked in the mutant (Fig. 5B). Self pollination was rare because shortened stamen filaments placed the anther below the receptive stigma (Fig. 5A) and because anther dehiscence was impaired (Fig. 5, C–F). Pollen appeared morphologically normal in mechanically opened anthers, and seeds appeared to develop normally if self pollination was assisted. All features were corrected by transforming the mutant with the cosmid containing *KOR* (Fig. 5A).

The *rsw1rsw2* double mutant had constitutively shortened roots (Fig. 6A) and at 31°C it showed: roots that swelled more than those of either single mutant (Fig. 6A); highly swollen dark grown hypocotyls with severely distorted cell shapes (Fig. 6B); incompletely differentiated stomata on cotyledons (Fig. 6C); and very distorted leaf surfaces (Fig. 6D). When plants were grown at 20°C until they bolted, no secondary bolts regenerated if the bolts were cut off and the plant transferred to 30°C even though a large rosette grown at the permissive temperature was available to support regrowth. Both single mutants successfully regenerate bolts in the same conditions (Williamson et al., 2001 for *rsw1*; unpublished data for *rsw2*).

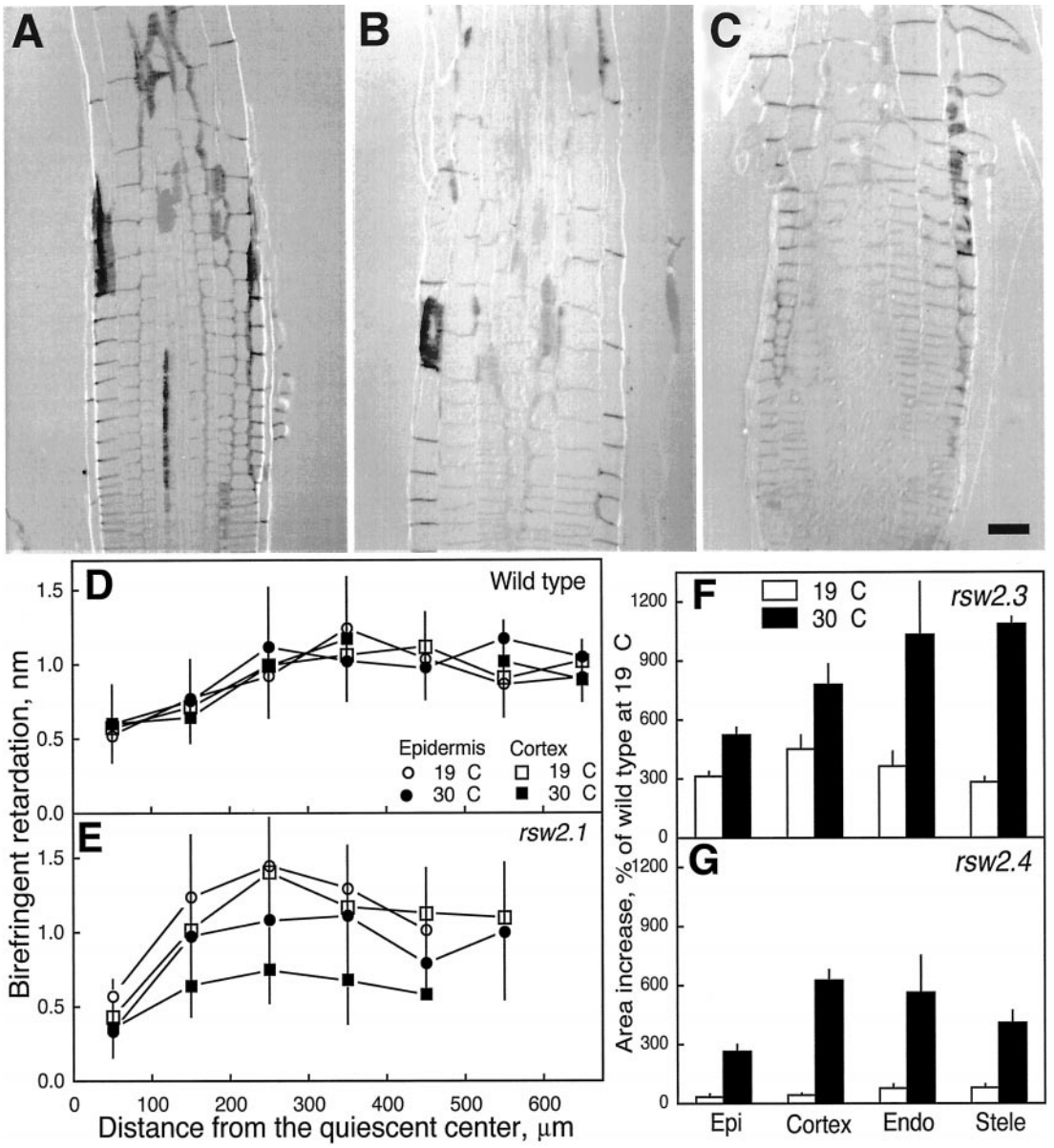

Figure 3. Characterization of radial swelling in *rsw2*: cell wall birefringent retardation and swelling in different tissues. A through C, Longitudinal sections of seedling roots viewed through polarized light optics for wild type grown at 19°C (A), *rsw2-4* grown at 19°C (B), and *rsw2-4* transferred to 30°C for 12 h (C). In plane cell walls with transverse microfibrils appear darker than the background and are seen in wild type and mutant at 19°C but only in the epidermis of the mutant at 30°C. Scale bar = 25 μm. D and E, Birefringent retardation versus distance from the quiescent center in the epidermal and cortical longitudinal cell walls of wild type (D) and *rsw2-1* (E). White symbols show data for plants grown at 19°C, black symbols show data for plants transferred to 30°C for 12 h. Circles show epidermis, squares show cortex. Data are means ±SE of 5 to 30 measurements from sections of four different roots. F and G, Extent of radial swelling of the major tissues of *rsw2-3* and *rsw2-4*. The increase in area of the tissue after 24 h at 19°C or 30°C is expressed as a percentage of the initial area of the same tissue in wild type. The data are means ± SE for measurements of four roots with the data from each root averaged from four sections. Note that *rsw2-3* was considerably swollen even at the permissive temperature and that in both alleles, all tissues became swollen but with swelling of the epidermis being less than the swelling of any other tissue.

DISCUSSION

RSW2 and *KOR* Are Allelic

Four findings support the view that *KOR* and *RSW2* are allelic: Both *rsw2* (this report) and *kor1* (Nicol et al., 1998) map just south of nga 129 on chromosome 5; an 8.5 kB genomic cosmid carrying *KOR* corrects all aspects of the Rsw2$^-$ phenotype; three *rsw2* alleles show different point mutations in the coding region of *KOR*; and the F_1 from crossing any of the *rsw2* alleles to *kor-1* gives a temperature-sensitive mutant phenotype albeit one that is milder than that seen in plants homozy-

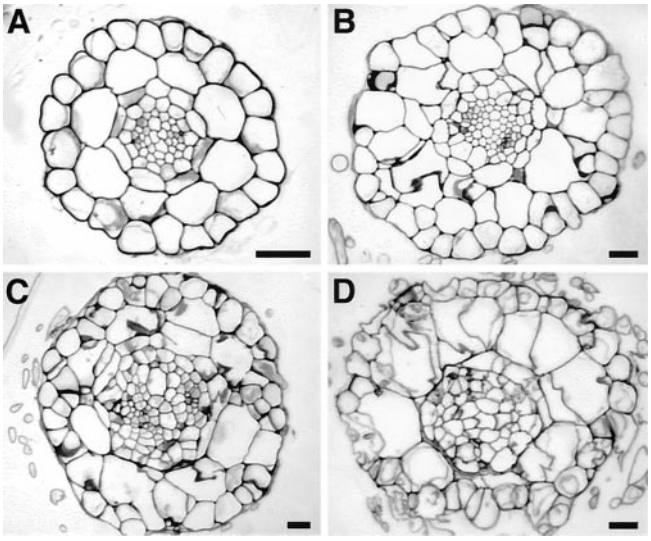

Figure 4. Additional cells and abnormal cell walls in cross-sections of wild type and *rsw2* mutants. Wild type (A), *rsw2-3* at 19°C (B), *rsw2-3* at 30°C for 24 h (C), *rsw2-4* at 30°C for 24 h (D). Scale bars = 25 μm. *rsw2-3* shows constitutive changes as well as a temperature sensitive component. Note that the magnification of the wild-type roots is nearly double that of the mutant roots.

gous for a temperature-sensitive *rsw2* allele. The new alleles with point mutations in the coding region of the KOR endo-1,4-β-glucanase add to the previously described promoter-defective *KOR* alleles. *kor-1* has a T-DNA insert 200 bp upstream of the ATG-initiation codon that lowers mRNA levels (Nicol et al., 1998) and produces low protein levels (Nicol et al., 1998; Zuo et al., 2000). *kor-2* is a stronger allele with almost undetectable levels of mRNA and protein as a result of a 1-kb deletion encompassing the promoter region and 5′-untranslated region (Zuo et al., 2000).

Cellulose Production Requires the KOR Endo-1,4-β-Glucanase

Four features of *rsw2* mutants implicate the KOR endo-β-1,4 glucanase in producing cellulose for primary cell walls (with the situation in secondary walls undetermined). First, roots of *rsw2-1* show specific, temperature-dependent cellulose reductions (Peng et al., 2000). Second, shoots (but not roots) of *rsw2-1* accumulate a readily extractable β-1,4-glucan (this report). Both features are shared with *rsw1* (Arioli et al., 1998; Peng et al., 2000). Third, birefringent retardation falls in extending cell walls of *rsw2* consistent with reduced cellulose production (Peng et al., 2000) and perhaps impaired alignment as occurs in *rsw1* (Sugimoto et al., 2001). Fourth, seedlings of the *rsw1rsw2* double mutant make significantly less cellulose than do seedlings of either of the single mutants. The firm linkage to cellulose production refines the initial studies of *kor-1*, which concluded that changes occurred in the cellulose/hemicellulose network (Nicol et al., 1998) and agrees with more recent studies of *kor-1* using Fourier transform infra-red spectroscopy (M. Fagard, G. Mouille, T. Desnos, F. Goubet, M. Lahaye, S. Vernhettes, M. McCann, and H. Höfte, submitted data). How RSW1 and KOR interact in producing cellulose cannot yet be firmly

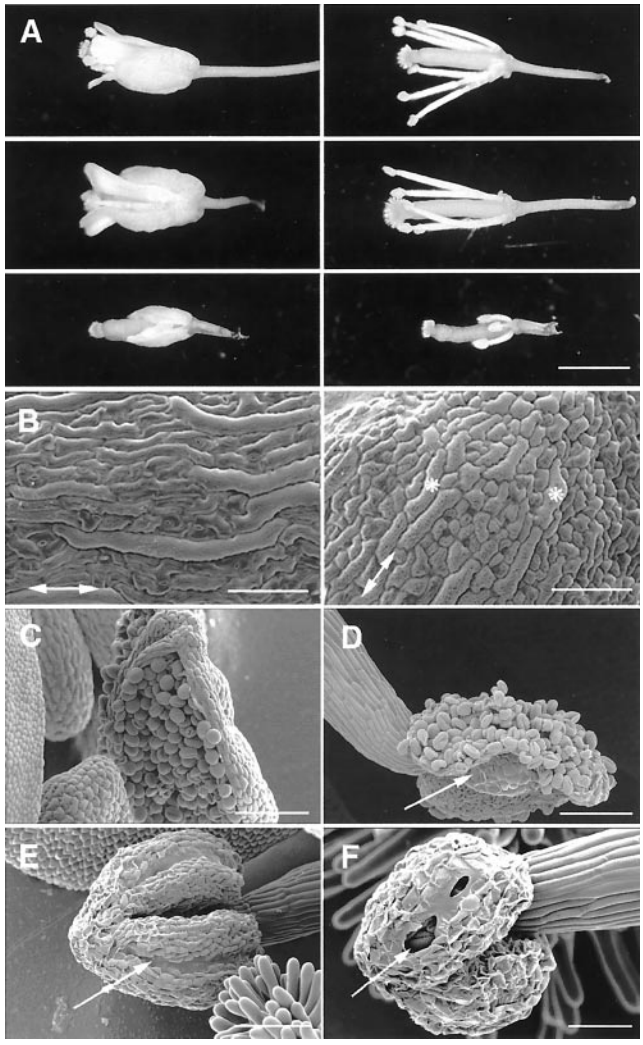

Figure 5. Floral abnormalities in *rsw2-1* seen in plants transferred from 20°C to 31°C after bolting. A, Changes in the relative lengths of floral organs. Whole flowers (left) and petals and sepals removed (right). Columbia wild type (top); *rsw2-1* complemented with *KOR* (middle); *rsw2-1* (bottom). Petals, sepals, and stamen filaments are much shorter in the mutant than in wild type so that the receptive stigma protrudes beyond them in the mutant. All traits are corrected by transformation with *KOR*. B, The mixture of long and short cells characteristic of the wild-type sepal (left) is much less marked in sepals of *rsw2-1* (right). Double-headed arrows show the long axis of the sepal. Asterisks show the slightly elongated cells in the mutant. C through F, Impaired anther dehiscence. The wild-type anther splits cleanly along the stomium before its surface cells visibly dessicate (C) and the anther wall folds right back as asymmetric shrinkage of the endothecial cells begins (D). *rsw2-1* anthers, in contrast, fail to split along their stomium (arrow) even when shrinkage of epidermal cells has begun (E) but partial splitting may follow when epidermal cell shrinkage is extreme (F). Scale bars = 1 mm (A), 100 μm (B–E), 50 μm (F).

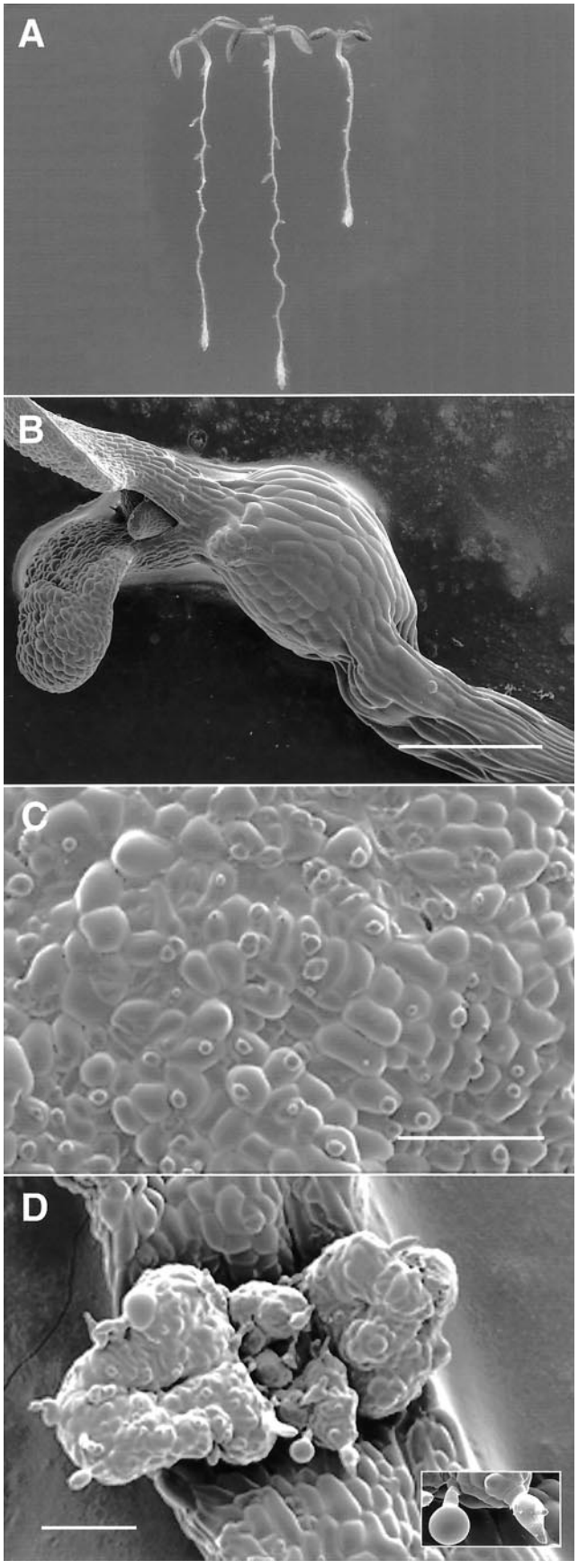

settled with the double mutant. When loss of gene function is incomplete at 31°C (the likely situation in *rsw1rsw2-1*), the observed additive phenotype can result from incomplete loss of function at two steps in a single pathway as well as from independent pathways, an interpretation that would be favored if null alleles were being used (Martienssen and Irish, 1999). However, the behavior at 19°C is particularly interesting in the present case. A constitutive root growth phenotype (Fig. 6) results from combining alleles at two loci, which individually support growth at wild-type rates (Baskin et al., 1992). This is most easily explained as the presence of the two gene products on the same pathway leading to cellulose production and growth.

Arabidopsis mutants now link cellulose deposition to genes encoding several closely similar glycosyltransferases (Arioli et al., 1998; Taylor et al., 1999; Fagard et al., 2000; Peng et al., 2000; Taylor et al., 2000) and an endo-1,4-β-glucanase (Nicol et al., 1998; Peng et al., 2000; this report). There are striking parallels with *Agrobacterium tumefaciens*, which also requires a glycosyltransferase (celA) and an endo-1,4-β-glucanase (celC) to make cellulose (Matthysse et al., 1995b). Matthysse et al. (1995a) proposed that celC transfers cello-oligosaccharides from a lipid-linked form to extend the glucan chain, but further work is needed to clarify the reaction pathway in both bacteria and plants.

The Rsw2$^-$ Morphological Phenotype

Nicol et al. (1998) noted the general similarity of the *kor-1* seedling phenotype to the cellulose deficient Rsw1$^-$ seedling phenotype. Various features of the Kor-1$^-$ phenotype in mature plants (e.g. reduced leaf and stem sizes) are now also known to be part of Rsw1$^-$ (Williamson et al., 2001). The new temperature-sensitive *rsw2* alleles show the main features of Kor-1$^-$ (Nicol et al., 1998) such as radial swelling in root and hypocotyl, reduced axial growth, and smaller leaves, stems, and flowers. Sepals and petals are more severely reduced in *rsw2* than in *rsw1* (Williamson et al., 2001), whereas seed set seems less severely affected but impaired anther dehiscence is a

Figure 6. Phenotype of the *rsw1rsw2-1* double mutant seen by light microscopy (A) and cryoscanning electron microscopy (B–D). A, Roots of the double mutant (right) show constitutive shortening and undergo more pronounced radial swelling than *rsw1* (left) and *rsw2* (center). Five days at 21°C, 2 d at 31°C. B, The hook region of the dark grown hypocotyl swells markedly when seedlings are transferred from 21°C to 31°C for d 3 to 6. The original diameter of the hypocotyl can be seen basal to the swelling. C, Surface of a cotyledon grown in the light at 31°C showing the highly simplified shapes of the epidermal cells and the failure of most stomata to develop a pore. D, The lamina surface of the unexpanded pair of first foliage leaves becomes highly irregular and trichomes (inset) are swollen and show reduced branching. Scale bars = 500 μm (B), 200 μm (C and D).

surprising aspect of Rsw2$^-$, which is not seen in Rsw1$^-$ (Williamson et al., 2001). Dehiscence involves breakdown of the septum separating adjacent locules, splitting of the stomium where the locules join, and opening of the split as the anther wall folds back (Dawson et al., 1993; Sanders et al., 1999). KOR defects could impair cell wall weakening, a function proposed for endocellulases secreted to the anther cell wall (Lashbrook et al., 1994; Neelam and Sexton, 1995). Alternatively and in keeping with the proposed role of KOR in cellulose synthesis, we are investigating whether KOR is needed to synthesize cellulose in the wall ridges that are deposited in endothecial cells just before anther dehiscence (Dawson et al., 1993; Bowman, 1994; Owen and Makaroff, 1995; Sanders et al., 1999). The location of the ridges is held to cause the differential shrinkage when endothecial cells dehydrate, expanding the initial split in the stomium. With impaired cellulose deposition in the ridges, the stomium may therefore not experience enough force to expand the opening and release pollen.

Further differences between *rsw2* and *rsw1* occur in roots. The two temperature sensitive alleles examined (*rsw2-3* and *rsw2-4*) contain extra cells, and some cell walls are incomplete and follow irregular paths. In this, the temperature-sensitive alleles resemble the strong *kor-2* allele (Zuo et al., 2000) rather than the weaker *kor-1* allele (Nicol et al., 1998). However, scanning electron microscopy of aerial parts of plants homozygous for *rsw2-1* has not shown obvious cell division abnormalities and the mutants do not show the massive disorganization of morphogenesis that characterizes *kor-2* (Zuo et al., 2000). The abnormal and incomplete cell plates seen in the roots plausibly result from a deficiency in cellulose synthesis. Dichlorobenzonitrile, the cellulose synthesis inhibitor, produces incomplete and wavy cell plates (Buron and Garcia-Herdugo, 1983; Venverloo et al., 1984; Gonzalez-Reyes et al., 1986; Mineyuki and Gunning, 1990; Vaughn et al., 1996). Cellulose is deposited in the cell plate at quite a late stage (Samuels et al., 1995) and the observations with dichlorobenzonitrile and with *rsw2* suggest that cellulose may be required to straighten the nearly mature cell plate. Extra rounds of division may ensue if faulty cytokinesis does not properly isolate daughter cells. Extra divisions do not occur in *rsw1* (T.I. Baskin, unpublished data; Sugimoto et al., 2001) so they are not simply a response to partition the extra volume produced by radial swelling.

Zuo et al. (2000) further supported a role for KOR in cytokinesis by showing that KOR is targeted to the cell plate in tobacco BY2 cells. They also demonstrated that transformation with a *KOR* gene that lacks targetting sequences, can restore the elongation defect without restoring the cytokinetic defect. Several features of the temperature-sensitive alleles also suggest it is unlikely that KOR only acts in cell plates: Expansion of cotyledons and hypocotyls is restricted even though cells in these organs would not divide during the period after germination when they are exposed to the restrictive temperature (Tsukaya et al., 1994; Mansfield and Briarty, 1996; Gendreau et al., 1997); birefringence in radial longitudinal walls is reduced well back into the expansion only zone of roots; a 56% reduction in total root cellulose (Peng et al., 2000) seems to be too large to reflect only defects in cell plates.

Most features of the *rsw1rsw2-1* double mutant are more severe manifestations of defects seen in both single mutants, but three features deserve note. First, slow root extension becomes constitutive in the double mutant, whereas extension rates in the single mutants are not significantly different from wild-type rates (Baskin et al., 1992). Second, enhanced radial swelling develops at the restrictive temperature in line with the more severe reduction in cellulose production that occurs in the double mutant. Third, regeneration of bolts is absolutely blocked when the double mutant is transferred to the restrictive temperature after bolting is initiated.

CONCLUSIONS

We have experimentally linked a second putative enzyme activity to cellulose production in Arabidopsis so that enzymes paralleling both *Agrobacterium* celA (glycosyltransferase) and celC (endo-1,4-β-glucanase) are now implicated. Detailed characterization of biochemical traits in the single and double mutants may show how the steps catalyzed by the two enzymes are related in vivo.

MATERIALS AND METHODS

Mutants

The *rsw1*, *rsw2-1*(Baskin et al., 1992), and *kor-1* (Nicol et al., 1998) mutants of Arabidopsis have been described. Three additional radial swelling mutants isolated in the same screen (Baskin et al., 1992) were assigned to the *rsw2* complementation group because roots of F_1 plants from crosses with *rsw2-1* showed temperature sensitive radial swelling. All mutants involve recessive, Mendelian factors. The F_1 progeny from complementation crosses to *kor-1* were compared with the F_1 from crossing *rsw2* with the Wassilewskija ecotype, the background for *kor-1*. Putative double homozygous mutants (*rsw1rsw2-1*) were selected in the F_2 on the basis of severe root phenotypes and their genotypes confirmed by showing that all progeny from crosses to *rsw1* and *rsw2-1* were Rsw$^-$. Baskin et al. (1992) described standard growth conditions on agar and soil, and any variations are noted in individual experiments.

Molecular Methods

For mapping, *rsw2-1* was crossed with the W9 marker line and deviation from 9:3:3:1 segregation in F_2 phenotypes assessed with the χ^2 test. DNA extracted by the

CTAB method from Rsw2$^-$ plants selected from an F_2 population after crossing *rsw2-1* (Columbia background) with the Landsberg *erecta* ecotype was tested with the cleaved amplified polymorphic markers *DFR* (Shirley et al., 1992) and *LEAFY3* (Weigel et al., 1992). The simple sequence length polymorphism marker nga 129 (Bell and Ecker, 1994) was tested on DNA extracted from one or two leaves of 3-week-old plants (Konieczny and Ausubel, 1993). The nga 129 PCR products of 177-bp (Columbia) and 179 (Landsberg) and ROX 350 size markers (ABI, Foster City, CA) were resolved on 4% or 6% (v/v) polyacrylamide gels using ABI Genescan software operating on an ABI 373 sequencer. Fragments were fluorescently labeled with 6-Fam through the 3′ nucleotide of the reverse primer. *rsw2-1* was transformed by vacuum infiltration (Bechtold et al., 1993) with the 8.5-kb genomic DNA fragment containing *KOR* (Nicol et al., 1998) and screened as described in Arioli et al. (1998).

Cell Wall Polysaccharides

The plant material, fractionation scheme for noncellulosic polysaccharides and carbohydrate analyses have been described (Peng et al., 2000). In brief, seedlings of Arabidopsis ecotype Columbia wild-type and *rsw2* were grown for 7 d at either 21°C or, to express their radial swelling phenotype (Baskin et al., 1992), at 21°C for 2 d followed by 31°C for 5 d. A crude cell wall pellet prepared from either shoots or from whole seedlings was successively extracted with chloroform/methanol (to remove lipids), with dimethylsulfoxide (starch), with ammonium oxalate (pectins), and with 0.1 and 4 M potassium hydroxide (hemicelluloses). Glycosidic linkage patterns were obtained by methylation analysis and monosaccharide composition of the various fractions after acid hydrolysis was determined by gas chromatography/mass spectrometry (GC/MS) of alditol acetates. Uronic acids were determined colorimetrically.

Readily extracted glucan was purified from the ammonium oxalate fraction of shoots by precipitating pectins with CTAB and from the neutralized and dialysed KOH fractions by centrifuging at 14,000*g* for 1 h. It was quantified by GC/MS measurement of alditol acetates of the Glc released by TFA. Samples of glucan purified from whole seedlings were subject to methylation analysis. Glucan (532 μg in 1.1 mL) was digested for 48 h at 37°C with: 0.5 units of endo-β-1,4-glucanase (endo-cellulase, EC 3.2.1.4; *Trichoderma*) from Megazyme International Ireland Ltd (Wicklow, Ireland) in 50 mM sodium acetate pH 4.7; 26.1 units of α-amylase (EC 3.2.1.1; porcine pancreas) from Sigma (St. Louis, MO) in 50 mM phosphate buffer pH 7. Supernatants (2,100*g*, 15 min) from the enzyme digest were lyophilized and alditol acetates analyzed by GC/MS without acid hydrolysis. (Endo-cellulase showed negligible activity toward starch or laminaran, and α-amylase showed negligible activity toward cellobiose or cello-oligosaccharides.)

Cellulose was estimated as TFA-insoluble material in single and double mutants. Seeds of *rsw1*, *rsw2-1*, and the *rsw1rsw2-1* double mutant were grown under standard conditions on agar (Baskin et al., 1992) for either 7 d at 21°C or 2 d at 21°C followed by 5 d at 31°C. Approximately 50 mg of whole seedlings were weighed, freeze-dried, and reweighed. Dried samples were ground to a fine powder by shaking for 6 s in a ball mill (SDI ULTRAMAT, Southern Dental Industries, Bayswater, Victoria). The mill capsule was then washed (6 × 0.75 mL) with ice-cold potassium phosphate buffer (0.5 M, pH 7) and mixed for 2 s for each wash. The combined washes were spun at 3,500 rpm for 10 min. The pellet was rinsed twice with deionized water before being dispersed in methanol/chloroform (5 mL 1:1, v/v). Samples were incubated at 37°C for 15 min, centrifuged, and the pellet dispersed in methanol/chloroform (5 mL), incubated for 30 min at 37°C, centrifuged, and the supernatant discarded. The pellet was then washed successively with methanol, acetone, and twice with deionized water (3 mL each). The non-cellulosic polysaccharides in the pellet were hydrolyzed with 2 M TFA (2 mL) at 120°C for 1 h. After centrifugation and water washes (2 × 1 mL), the cellulose pellet was removed. The cellulose pellet was washed twice with acetone, dried at 65°C for 15 min, and dispersed in 72% (v/v) H_2SO_4 (100 μL) with sonication for 30 to 60 min. The mixture was diluted with deionized water (2 mL) and the samples hydrolyzed at 100°C for 2 h. After cooling, *myo*-inositol (the internal standard) was added, thoroughly mixed, and centrifuged. An aliquot (0.5 mL) of the supernatant was then neutralized with 0.2 M $Ba(OH)_2$ (1 mL), followed by a spatula tip-full of $BaCO_3$ and enough 0.2 M $Ba(OH)_2$ to adjust the pH to 7. Samples were centrifuged for 10 min, the supernatants freeze-dried, and neutral sugars converted to alditol acetates and analyzed by GC/MS (Peng et al., 2000).

Microscopy

Morphological features were documented on fresh material with a Wild Heerbrug Photomakroscop M400. For cryoscanning electron microscopy, fresh samples attached with tissue freezing medium to a mounting plate were plunged into liquid nitrogen slush at −230°C. The plate was inserted into the preparation chamber of an Oxford CT1500 Cryo Preparation System and slowly warmed to −80°C to remove surface ice crystals. The specimen, coated with 10 nm of gold, was transferred to the cryostage (−185°C) of a S360 scanning electron microscope (Cambridge Instruments; Cambridge, UK). For light microscopy, seedling roots were embedded without shrinkage (data not shown) in butyl-methyl-methacrylate (Baskin and Wilson, 1997). Serial transverse sections of the apical 600 μm of four roots for each treatment were stained with periodic acid-Schiff's reagent. Tissue areas and cell numbers were measured in the four sections showing the largest root diameters. Tissue boundaries were traced with the cursor on digital images and areas computed by Image 1/AT (Universal Imaging, West Chester, PA). Cell numbers are expressed as mean ± SE for the 16 determinations. Polarized light microscopy was conducted on radial-longitudinal cell walls in 2-μm median longitudinal methacrylate sections of roots and birefringent retardation measured photometrically as described by Baskin et al. (1999).

ACKNOWLEDGMENTS

We thank Jan Wilson and Ann Cork for excellent technical assistance.

Received November 15, 2000; returned for revision December 5, 2000; accepted February 13, 2001.

LITERATURE CITED

Arioli T, Peng L, Betzner AS, Burn J, Wittke W, Herth W, Camilleri C, Höfte H, Plazinski J, Birch R et al. (1998) Molecular analysis of cellulose biosynthesis in *Arabidopsis*. Science **279:** 717–720

Baskin TI, Betzner AS, Hoggart R, Cork A, Williamson RE (1992) Root morphology mutants in *Arabidopsis thaliana*. Aust J Plant Physiol **19:** 427–437

Baskin TI, Meekes HTHM, Liang BM, Sharp RE (1999) Regulation of growth anisotropy in well-watered and water-stressed maize roots: II. Role of cortical microtubules and cellulose microfibrils. Plant Physiol **119:** 681–692

Baskin TI, Wilson JE (1997) Inhibitors of protein kinases and phosphatases alter root morphology and disorganize cortical microtubules. Plant Physiol **113:** 493–502

Bechtold N, Ellis J, Pelletier G (1993) In planta *Agrobacterium*-mediated gene transfer by infiltration of adult *Arabidopsis thaliana*. Comptes Rendue Acad Sci Ser III Sci de la Vie **316:** 1194–1199

Bell CJ, Ecker JR (1994) Assignment of 30 microsatellite loci to the linkage map of *Arabidopsis*. Genomics **19:** 137–144

Bowman JL (1994) Arabidopsis: an atlas of morphology and development. Springer-Verlag, New York

Buron MI, Garcia-Herdugo G (1983) Experimental analysis of cytokinesis: comparison of the effects of inhibition induced by 2,6-dichlorobenozonitrile and caffeine. Protoplasma **118**: 192–198

Carpita NC, Shea EM (1989) Linkage structure of carbohydrates by gas chromatography mass spectrometry (GC-MS) of partially methylated alditol acetates. *In* CJ Biermann, GD McGinnis, eds, Analysis of Carbohydrates by GLC and MS. CRC Press, Boca Raton, FL, pp 157–216

Dawson J, Wilson ZA, Aarts MGM, Braithwaite AF, Briarty LG, Mulligan BJ (1993) Microspore and pollen development in 6 male-sterile mutants of *Arabidopsis thaliana*. Can J Bot **71:** 629–638

Fagard M, Desnos T, Desprez T, Goubet F, Refregier G, Mouille G, McCann M, Rayon C, Vernhettes S, Höfte H (2000) *PROCUSTE1* encodes a cellulose synthase required for normal cell elongation specifically in roots and dark-grown hypocotyls of *Arabidopsis*. Plant Cell **12:** 2409–2423

Gendreau E, Traas J, Desnos T, Grandjean O, Caboche M, Höfte H (1997) Cellular basis of hypocotyl growth in *Arabidopsis thaliana*. Plant Physiol **114:** 295–305

Gonzalez-Reyes JA, Navas P, Garcia-Herdugo G (1986) An ultrastructural study of cell plate modifications induced by 2,6-dichlorobenzonitrile on onion root meristems. Protoplasma **132**: 172–178

Konieczny A, Ausubel FM (1993) A procedure for mapping *Arabidopsis* mutations using co-dominant ecotype-specific PCR-based markers. Plant J **4:** 403–410

Lashbrook CC, Gonzalezbosch C, Bennett AB (1994) Two divergent endo-β-1,4-glucanase genes exhibit overlapping expression in ripening fruit and abscising flowers. Plant Cell **6:** 1485–1493

Mansfield SG, Briarty LG (1996) The dynamics of seedling and cotyledon cell development in *Arabidopsis thaliana* during reserve mobilization. Int J Plant Sci **157:** 280–295

Martienssen R, Irish V (1999) Copying out our ABCs: the role of gene redundancy in interpreting genetic hierarchies. Trends Genet **15:** 435–437

Matthysse AG, Thomas DL, White AR (1995a) Mechanism of cellulose synthesis in *Agrobacterium tumefaciens*. J Bacteriol **177:** 1076–1081

Matthysse AG, White S, Lightfoot R (1995b) Genes required for cellulose synthesis in *Agrobacterium tumefaciens*. J Bacteriol **177:** 1069–1075

Mineyuki Y, Gunning BES (1990) A role for the preprophase band of microtubules in maturation of new cell wall, and a general proposal on the function of preprophase band sites in cell division of higher plants. J Cell Sci **97:** 527–537

Neelam A, Sexton R (1995) Cellulase (endo-β-1,4 glucanase) and cell wall breakdown during anther development in the sweet pea (*Lathyrus odoratus* L.): isolation and characterization of partial cDNA clones. J Plant Physiol **146:** 622–628

Nicol F, His I, Jauneau A, Vernhettes S, Canut H, Höfte H (1998) A plasma membrane-bound putative endo-1,4-β-D-glucanase is required for normal wall assembly and cell elongation in *Arabidopsis*. EMBO J **17:** 5563–5576

Owen HA, Makaroff CA (1995) Ultrastructure of microsporogenesis and microgametogenesis in *Arabidopsis thaliana* (L.) Heynh. ecotype Wassilewskija (Brassicaceae). Protoplasma **185:** 7–21

Pear JR, Kawagoe Y, Schreckengost WE, Delmer DP, Stalker DM (1996) Higher plants contain homologs of the bacterial *celA* genes encoding the catalytic subunit of cellulose synthase. Proc Nat Acad Sci USA **93:** 12637–12642

Peng L, Hocart CH, Redmond JW, Williamson RE (2000) Fractionation of carbohydrates in *Arabidopsis* seedling cell walls identifies three radial swelling loci that are involved specifically in cellulose production. Planta **211:** 406–414

Richmond TA, Somerville CR (2000) The cellulose synthase superfamily. Plant Physiol **124:** 495–498

Samuels AL, Giddings TH Jr, Staehelin LA (1995) Cytokinesis in tobacco BY-2 and root tip cells: a new model of cell plate formation in higher plants. J Cell Biol **130:** 1345–1357

Sanders PM, Bui AQ, Weterings K, McIntire KN, Hsu YC, Lee PY, Truong MT, Beals TP, Goldberg RB (1999) Anther developmental defects in *Arabidopsis thaliana* male-sterile mutants. Sex Plant Reprod **11:** 297–322

Shirley BW, Hanley S, Goodman HM (1992) Effects of ionizing radiation on a plant genome: analysis of two

Arabidopsis transparent testa mutations. Plant Cell **4:** 333–347

Sugimoto K, Williamson RE, Wasteneys GO (2001) Wall architecture in the cellulose deficient *rsw1* mutant of arabidopsis: microfibrils but not microtubules lose their transverse alignment before microfibrils become unrecognisable in the mitotic and elongation zones of roots. Protoplasma (in press)

Taylor NG, Laurie S, Turner SR (2000) Multiple cellulose synthase catalytic subunits are required for cellulose synthesis in *Arabidopsis*. Plant Cell **12:** 2529–2539

Taylor NG, Scheible W-R, Cutler S, Somerville CR, Turner SR (1999) The *irregular xylem3* locus of *Arabidopsis* encodes a cellulose synthase required for secondary cell wall synthesis. Plant Cell **11:** 769–780

Tsukaya H, Tsuge T, Uchimiya H (1994) The cotyledon: a superior system for studies of leaf development. Planta **195:** 309–312

Vaughn KC, Hoffman JC, Hahn MG, Staehelin LA (1996) The herbicide dichlobenil disrupts cell plate formation: immunogold characterization. Protoplasma **194:** 117–132

Venverloo CJ, Goosen-de Roo L, van Spronsen PC, Libbenga KR (1984) Cell division in *Nautilocalyx* explants: III. Effects of 2,6-dichlorobenzonitrile on phragmosome, band of microtubules and cytokinesis. J Plant Physiol **116**: 225–234

Weigel D, Alvarez J, Smyth DR, Yanofsky MF, Meyerowitz EM (1992) *LEAFY* controls floral meristem identity in *Arabidopsis*. Cell **69:** 843–859

Williamson RE, Burn JE, Birch R, Baskin TI, Arioli T, Betzner AS, Cork A (2001) Morphology of *rsw1,* a cellulose-deficient mutant of *Arabidopsis thaliana*. Protoplasma (in press)

Zuo J, Niu QW, Nishizawa N, Wu Y, Kost B, Chua NH (2000) KORRIGAN, an *Arabidopsis* endo-1,4-β-glucanase, localizes to the cell plate by polarized targeting and is essential for cytokinesis. Plant Cell **12:** 1137–1152